GSA Data Repository Item **2013197** accompanies Averill, M.G., and Miller, K.C., 2013, Upper crustal structure of the southern Rio Grande rift: A composite record of rift and pre-rift tectonics, in Hudson, M.R., and Grauch, V.J.S., eds., New Perspectives on Rio Grande Rift Basins: From Tectonics to Groundwater: Geological Society of America Special Paper 494, p. 463–474, https://doi.org/10.1130/2013.2494(17).

Supplement to:

Upper Crustal Structure of the Southern Rio Grande Rift: A Composite Record of Rift and Pre-Rift Tectonics

Matthew G. Averill* and Kate C. Miller** (corresponding author)
Department of Geological Sciences, University of Texas at El Paso, El Paso, TX 79902.

**Present Address: Anadarko Petroleum Co., 1201 Lake Robbins Dr., P.O. Box 1330, Houston, TX 77251-1330, Email: Matthew.Averill@anadarko.com.*

***Present Address: Department of Geology and Geophysics, Texas A&M University, MS 3115 College Station, Texas 77843-3115, Email: kcmiller@tamu.edu.*

INTRODUCTION

Following is a brief summary of the technical details of the seismic data analysis, the result of which are the velocity models shown in figures 3 and 4 in the paper.

DATA ACQUISITION

The seismic data were acquired by the University of Texas at El Paso in May of 2003 along a 205 km transect across southern New Mexico and Far West Texas (Fig. 1). A total of 793 TEXAN seismic recorders were laid out at variable spacing of 100 m, 200 m, and 600 m along the length of the transect to record 8 explosive shots with an average spacing of 35 km. Seismic recorders were equipped with single-component 4-Hz vertical geophones. The greatest part of the transect was instrumented at 600 m spacing. Along a 50-km-long portion of the transect, centered on Potrillo Mountains, recorders were deployed at 100 m. An additional 57 instruments were deployed at 200 m spacing on the eastern end of the profile in a location that was also the subject of a site investigation for a desalination plant being built by the El Paso Water Utility. The seismic instruments recorded a total of 8 explosive shots ranging in size from 450 to 900 kg that were set off in holes 80 to 100 m deep holes. The resultant data and metadata are available from the IRIS Data Management Center and are discussed below.

DATA PROCESSING

Two seismic records (Fig. 2) illustrate the character and quality of the seismic data. First arrivals are distinguishable along the entire length of each shot gather except in the urbanized El Paso region where cultural noise overwhelms many of the arrivals. The steep slopes of first arrival travel times at offsets of less than 10 km results from energy propagating in low-velocity basin fill. The sharp increase in apparent velocities to greater than 5 to 6 km/s beyond 10 km offset, is indicative of a true Pg phase, the diving wave that travels in the crystalline upper crust. The pattern of local advances and delays in first arrival times along the records corresponds to the locations of mountain ranges and basins, respectively.

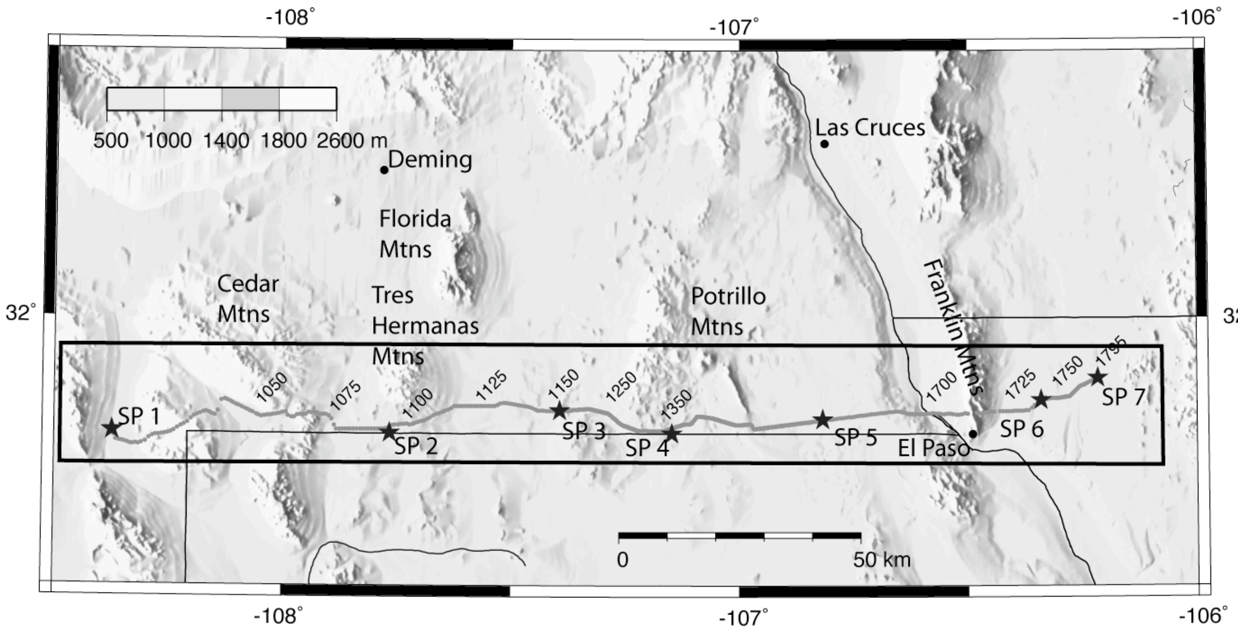

Figure 1. Location map for the seismic survey. Stars show shot point (SP) locations. Small gray dots are receiver locations. Black rectangle enclosing shot and receiver locations shows map view of model spaced used in the tomography.

A total of 4632 first arrival times were determined from the data. Uncertainties in the travel-times were determined using an automated scheme based on an empirical relationship between uncertainty values and signal-to-noise ratios (SNR) calculated within a 250 ms window (Zelt and Forsyth, 1994). The uncertainties range from as low as 20 ms for SNR of 10 to 150 ms for SNR less than 1.0. The average uncertainty was approximately 60 ms for first arrivals and 100 ms for reflected arrivals.

SEISMIC TOMOGRAPHY

For this study, we developed velocity models from the arrival times using a 3D first arrival tomography (Hole, 1992). In general, first-arrival tomography produces a smoothed velocity model that represents the minimum structure necessary to fit the travel-time data (Zelt et. al., 2003). We ran the seismic tomography using a 3-D velocity space in order to compensate for the crooked-line geometry of the profile. The model space was comprised of a 1 x 1 km grid with dimensions of 230 km length (X), 25 km width (Y), and 68 km height (Z). To obtain greater structural resolution, the model was also run with 0.5 km grid. For display purposes, we have created 2-D views of velocity structure by collapsing the model space through a weighted average of velocity in the Y-direction, based on ray coverage.

We developed a 1-D starting model by fitting a travel-time curve to all the first arrivals, with respect to absolute source-receiver offset, using the program MacR1D (Luetgert, 1992), which calculates travel-times based on a 1-D velocity-depth model. Steep velocity gradients in this initial model were then smoothed for the tomography in order to distribute ray paths more evenly within the initial model. A total of 4632 first arrival travel times were used in an inversion procedure that involved iteratively solving for changes to the velocity model 6 times consecutively for each of 5 smoothing operators. These operators were progressively reduced in

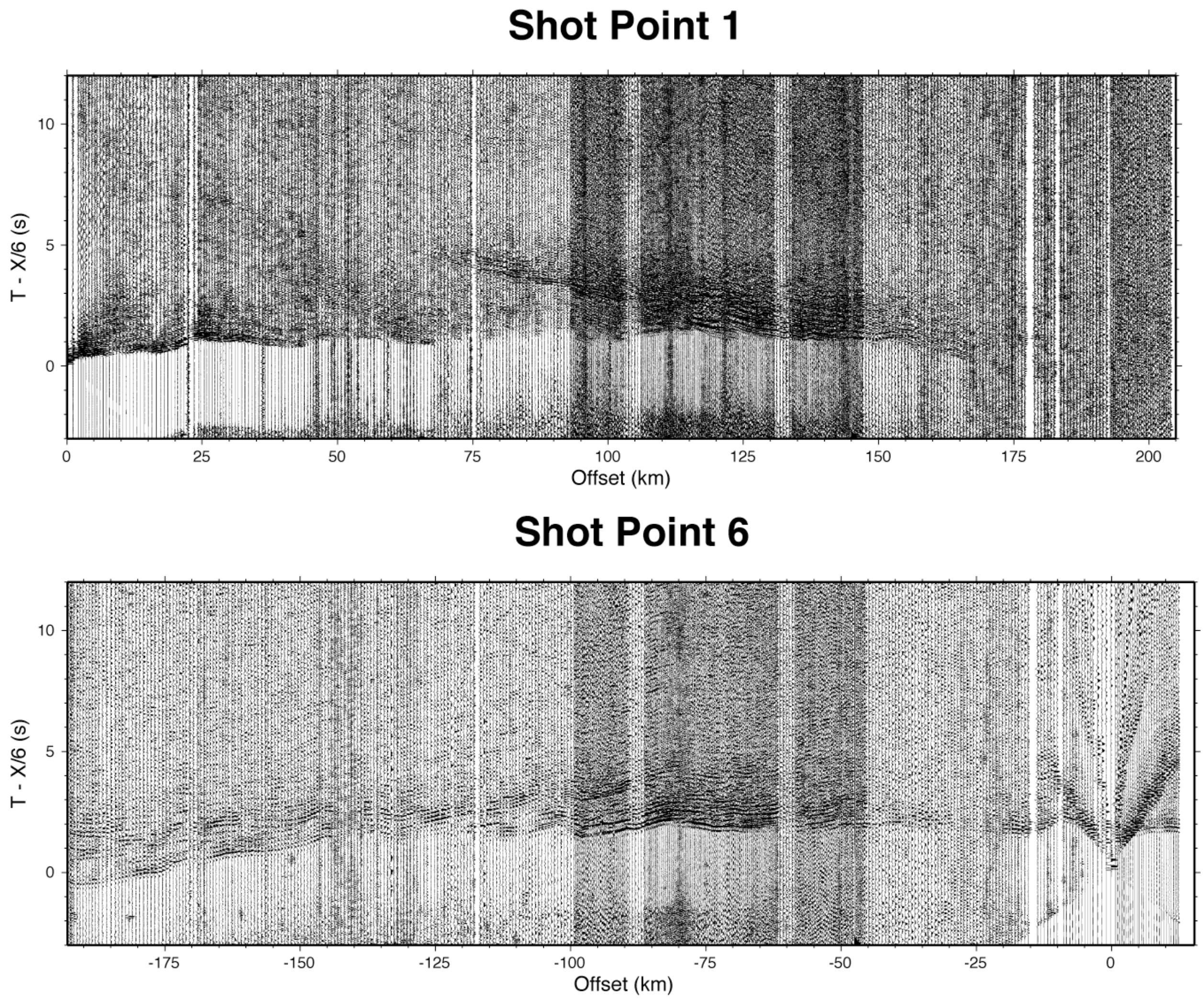

Figure 2. Example seismic record sections from shot points 1 and 6. Travel time (T) is reduced by the offset (X) divided by 6 km/s.

size from 96x24x24 km to 4x2x2 km. The final velocity model (Fig. 3) has an RMS travel-time misfit of 70 ms. We note that we tested a number of other 1-D initial models and were able to achieve travel-time misfits for each that were all less than an RMS value ca. ~120 ms. The 1D model we ultimately chose as a starting point was the one that produced the best ray coverage and the minimum travel-time misfit in the final iteration.

The geologic interpretation of the model hinges upon some understanding of the uncertainty in velocity values and the reliability of the velocity structure. These factors are controlled by ray coverage, travel time error and the smoothing parameters chosen in the inversion. The travel-time error can be characterized in terms of an individual travel-time misfit for each shot-receiver pair and an overall RMS for all travel-time residuals (Fig. 4). The overall RMS for the model is 70 ms, however, individual misfits are locally much higher. This calculated misfit is greater than the average empirically determined travel time uncertainty of approximately 60 ms and is less than the commonly accepted "picking" error of 100-150 ms. A plot of calculated and observed travel times combined with the travel-time residuals provides a qualitative understanding of the

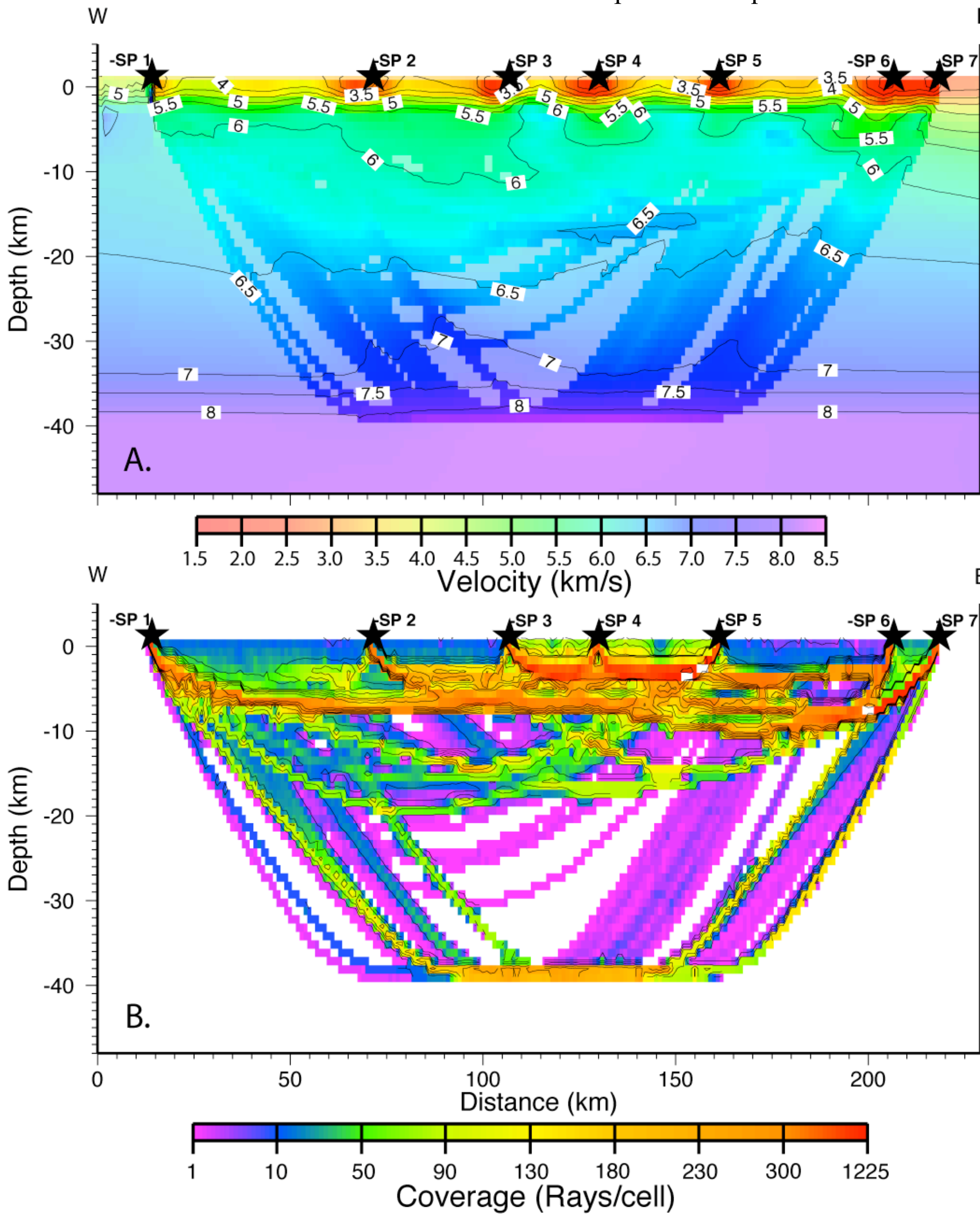

Figure 3. Final velocity model (A) and ray coverage (B) for 1 km grid. White areas are regions of no ray coverage.

reliability of different regions of the model (Fig. 4). In general, the highest misfits (> 200 ms) are observed at short source-receiver offsets (< 10 km) corresponding to a lack of reversing coverage caused by sparse source coverage and to ray paths traveling through low velocity basins. This occurs primarily because the inverse technique has an inherent difficulty in fitting the large velocity contrasts between low velocity basin sediments and adjacent high velocity basement rocks. In addition, high residuals travel times between 175 and 200 km in the model result from low signal-to-noise ratios for arrivals in urban El Paso.

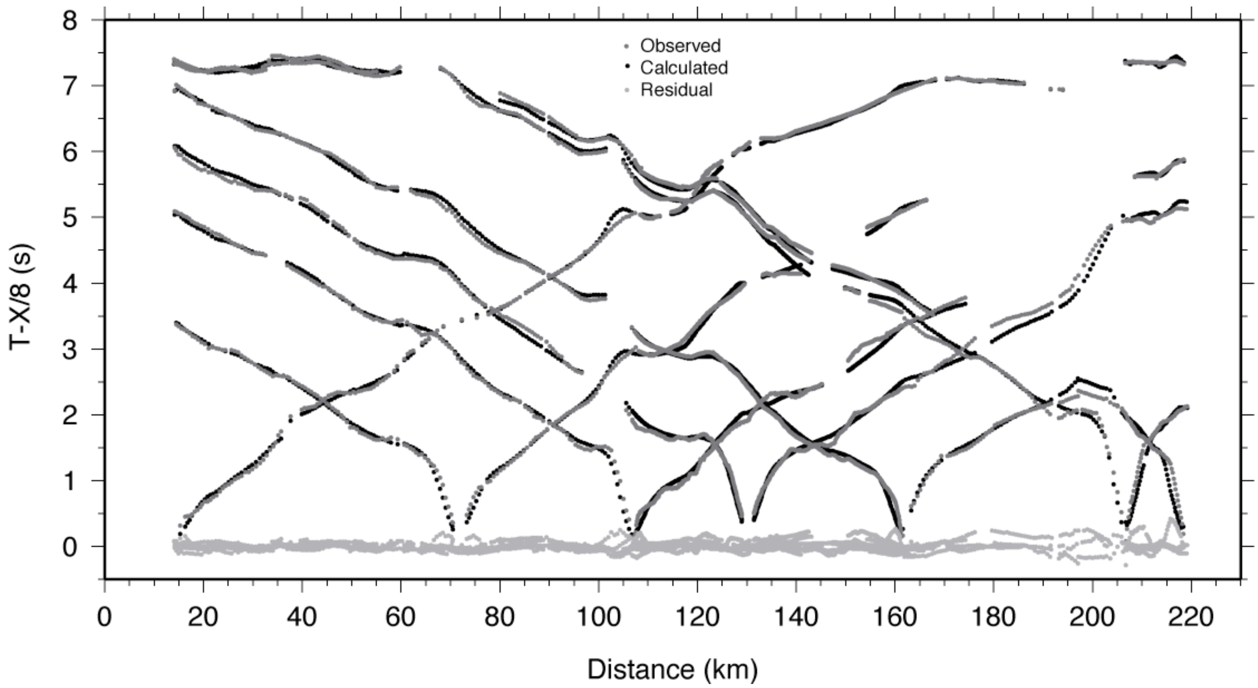

Figure 4. Graph of observed, calculated and residual travel times for final velocity model. Travel time (T) is reduced by the offset (X) divided by 8 km/s.

A ray coverage plot provides a qualitative view of regions of the model that are inherently most reliable (Fig. 3). In general, the more ray coverage there is in any given area of the model, the better the constraint is on the velocity in that area. Ray coverage in the upper 3 km is generally limited by the sparse shot spacing. The highest ray coverage occurs at depths between 3 and 8 km. Ray coverage is very high between shot points 3 through 5 where the receiver spacing was 100 to 200 m. The relative lack of arrival times between shot points 5 and 6 is the result of cultural noise in urban El Paso and results in reduced ray coverage in this part of the model (Fig. 4).

Checkerboard tests provide insight into both velocity uncertainty and structural reliability. We applied a checkerboard method similar to those commonly used for model resolution assessment (e.g., Hearn and Ni, 1994; Zelt and Forsyth, 1994; Vasco and Johnson, 1998). We ran checkerboard tests by adding a sinusoidal velocity perturbation of 5% with wavelengths of 10x5 and 20x10 km in the X and Z directions respectively to a 1D velocity model (Fig. 5). The checker sizes were chosen to be larger than the final smoothing operator of 4x2x2 km, because it puts a limit on the minimum size feature that can be resolved. Results for the 10x5 km checkerboard test show clear spatial recovery of the 5 percent velocity perturbations down to nearly 4 km depth (Fig. 6a). To a lesser extent, checkers with amplitudes of approximately 1.5

percent are recovered to 6 km depth. For the 20x10 km checkers, we see 5 percent velocity recovery and well resolved checkers to nearly 6 km depth and recovery of checkers with amplitudes of 1.5 percent to 12 km depth (Fig. 6b). These results show that absolute velocity values are most reliably recovered for features at least 10x5 km size within 10 km of each shot point and down to approximately 5 km depth.

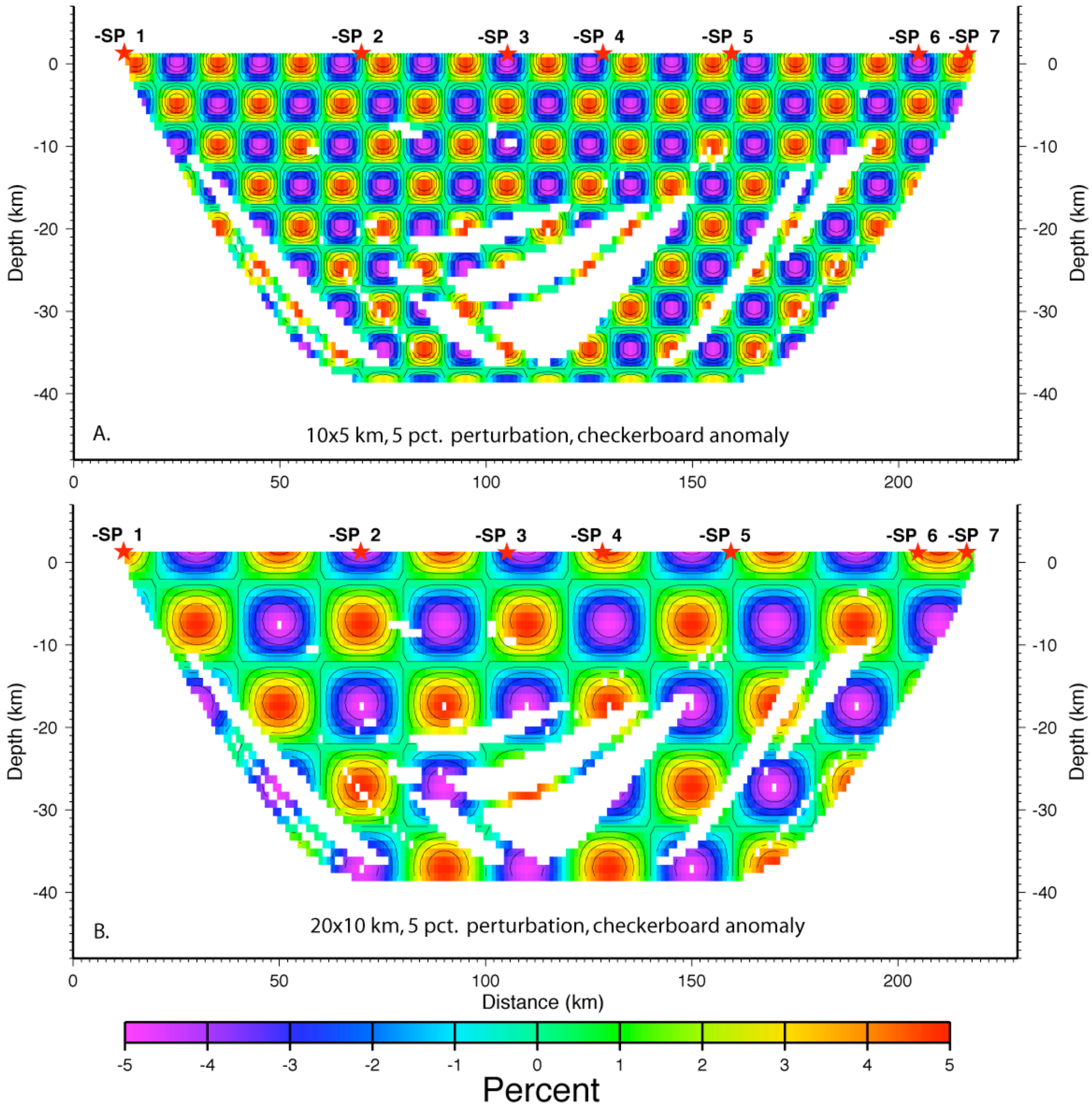

Figure 5. Original sinusoidal "checkers" that were added to a 1D velocity model to implement checkerboard test. White areas are regions of no ray coverage. A. Checkerboard with 5% perturbation in velocity with checker dimensions of 10x5 km. B. Checkerboard with 5% perturbation in velocity with checker dimensions of 20x10 km

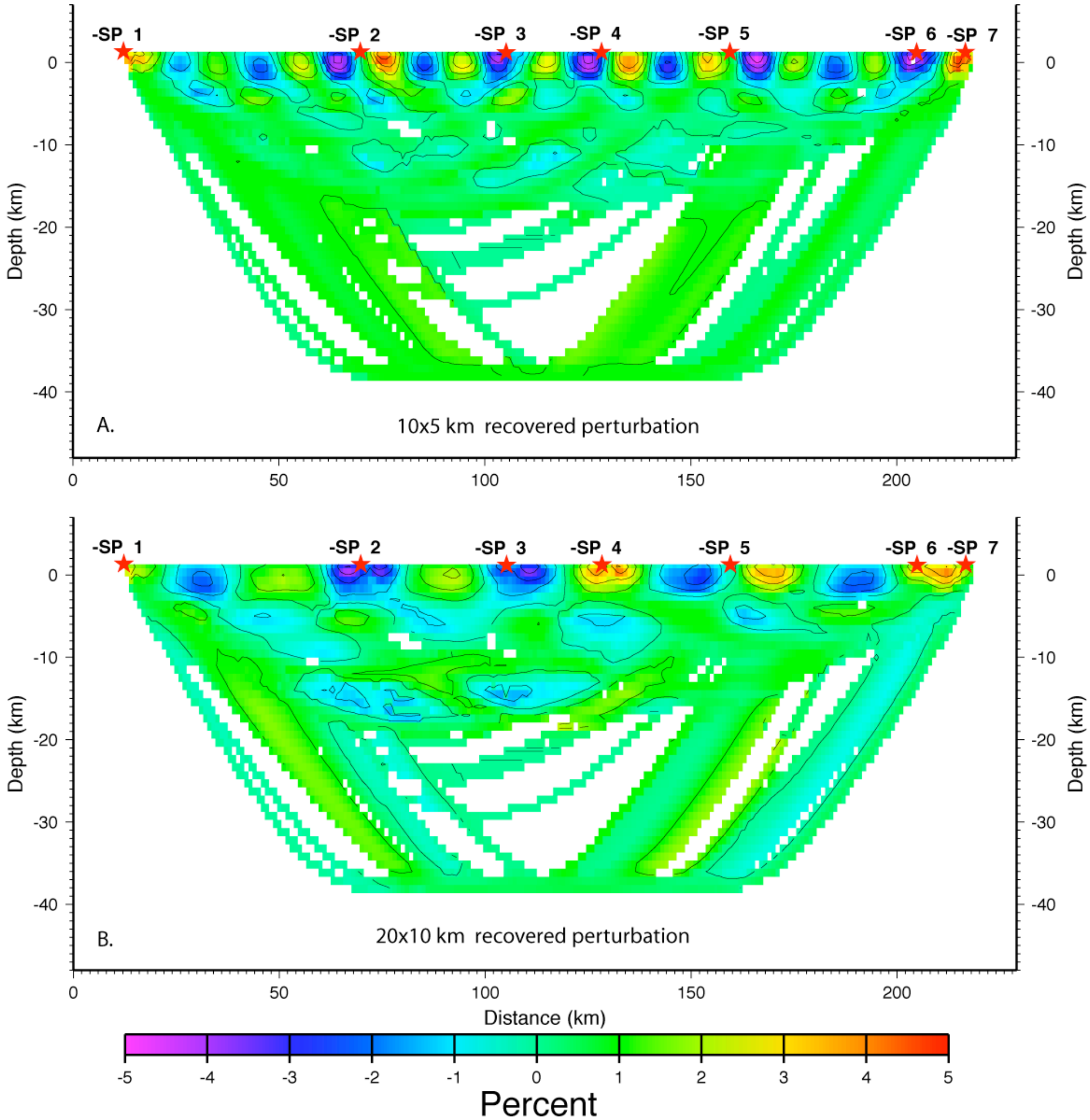

Figure 6. Recovered checkers after inversion of synthetic travel times through 1D model with 5% checkers added. A. Recovery of 10x5 km checkers. B. Recovery of 20x10 km checkers.

REFERENCES

Hearn, T.M., and Ni, J.F., 1994, Pn velocities beneath continental collision zones: the Turkish-Iranian Plateau: Geophysical Journal International, v. 117, p. 273-283.

Hole, J.A., 1992, Nonlinear high-resolution three-dimensional seismic travel time tomography: Journal of Geophysical Research, v. 97, p. 6553-6562.

Luetgert, J., 1992, MacRay-interactive two-dimensional seismic raytracing for the Macintosh: U.S. Geological Survey Open File Report 92-356, 43 pp.

Vasco, D.W., and Johnson, L.R., 1998, Whole earth structure estimated from seismic arrival times: Journal of Geophysical Research, v. 103, p. 2633-2671.

Zelt, C.A., and Forsyth, D.A., 1994, Modeling wide-angle seismic data for crustal structure Grenville province: Journal of Geophysical Research, v. 99, p. 11687-11704.

Zelt, C.A., Kalachand, S., Naumenko, J.V. and Sawyer, D.S., 2003, Assessment of crustal velocity models using seismic refraction and reflection tomography: Geophysical Journal International, v. 153, p. 609-626.